Innovative condenser - storage tank - concept for residential heat pumps

Kevin Diewald[1]*, Hannes Fugmann[1], Lena Schnabel[1],
Christiane Thomas[2]

[1]Fraunhofer-Institut for Solar Energy Systems, ISE
Heidenhofstraße 2, 79110 Freiburg, Germany
kevin.diewald@ise.fraunhofer.de

[2]TU Dresden, Schaufler Chair of Refrigeration, Cryogenics and Compressor Technology,
01062 Dresden, Germany

* Corresponding Author

ABSTRACT

Heat pumps for space heating and domestic hot water (DHW) supply have great potential for decarbonizing the building sector. In the European Union, the F-Gas Regulation on fluorinated greenhouse gases aims to reduce the use of HFC refrigerants. Natural refrigerants, especially R290, offer great potential for efficient operation, especially for heat pump applications. Heat pumps are available in a wide range for single-family houses (SFH) and small multi-family houses (MFH), therefore houses in urban areas are the focus of developments. In these areas the use of an air/water heat pump is not always possible due to the often dense population, the noise restrictions or the limited available space. For this reason, Fraunhofer ISE is investigating the combination of heat pumps and Photovoltaic thermal hybrid solar (PVT) collectors as a heat source.
The focus of this article is the heat pump system with the refrigerant cycle, the water storage tank, the heating, and the DHW circuit. An alternative concept is presented in comparison to the standard heat pump systems for heating and DHW. The goal of this system is to produce the DHW during normal heating mode without a special DHW mode. Particular attention is paid to the condenser of the heat pump, which can be designed as an immersed or mantle heat exchanger. The use of R290 makes the charge of refrigerant in the heat pumps a design criterion. Therefore, a detailed thermodynamic model of the heat pump is developed with the program language Modelica. The compressor and evaporator are fitted with data from the manufacturers to achieve realistic simulation results. The simulation results are used to design the condensers and to compare the two types with each other. The design parameters are the coefficient of performance (COP), the achievable DHW temperature in the upper part of the storage tank and the refrigerant mass.

1. INTRODUCTION

Heat pumps are gaining importance worldwide and in parts of Europe heat pumps are already the dominant solution for heating buildings. This article presents a heat pump storage concept that can generate domestic hot water (DHW) and space heating (SH) at the same time. In buildings, thermal storage tanks are used to store hot water (DHW or heating water) and can thus compensate load shifting. In conjunction with heat pumps, there are advantages in terms of operation, for example the number of start-stops can be reduced (Heinz et al., 2016). Monitoring results have shown that the DHW demand for single-family homes amounts to 5-30 % of the heat demand. The proportion depends on user behavior and the number of people, but also on the energy efficiency of the building. As the efficiency of the building increases (better insulation), the proportion of DHW increases, making the preparation of it more important (Günther et al., 2020). In general, two different storage tanks are installed, one for DHW and one for space heating, which are hydraulically connected to the heat pump. One way to reduce the installation effort is to use a combined storage tank that stores heat for both space heating and DHW. Heat is stored at DHW level in the upper part of the storage tank and at space heating level in the lower part. The storage tank is charged via hydraulic installations with 3-way valves and a circulation pump, which charges the upper or lower part as required (Haller et al., 2014).

2. SYSTEM DESCRIPTION

Figure 1 shows the system diagram of a conventional heat pump with a plate heat exchanger as a condenser, a combined storage tank, and the corresponding hydraulic components (3-way valves and circulation pump). When using a heat pump, a high-volume flow rate is required for charging the zones compared to fossil heat generators to keep the temperature difference across the condenser low and to achieve the highest coefficient of performance (COP) of the heat pump. However, the high-volume flow can lead to the stratification in the tank being destroyed i.e., the mixing between the DHW zone with higher temperatures and the space heating zone with lower temperatures. This would destroy the effect of the combined storage tank and special installations would again be required to preserve the stratification (Lerch et al., 2014). Heinz et al. (Heinz et al., 2016) consider another heat pump system with a combined storage tank in which the condenser is integrated as a coil heat exchanger in the storage tank. This approach is taken up and is further developed. Figure 2 shows the alternative heat pump storage concept that is being investigated in detail. The initial results from the simulation of the stationary processes in the system are presented in this paper. Compared to typical heat pump storage concepts, the condenser is integrated directly into the storage tank. Accordingly, refrigerant lines lead from the storage tank to the heat pump, in contrast to the usual hydraulic lines (Figure 1).

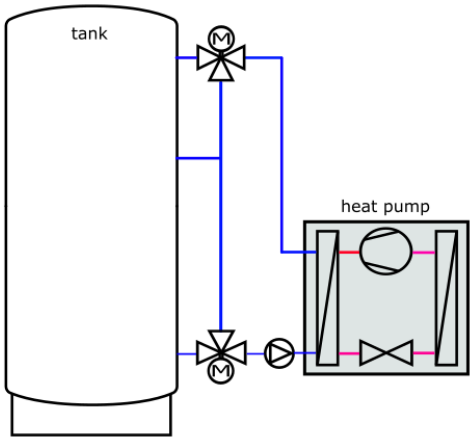

Figure 1: Conventional heat pump with combined storage tank and hydraulic connections (blue)

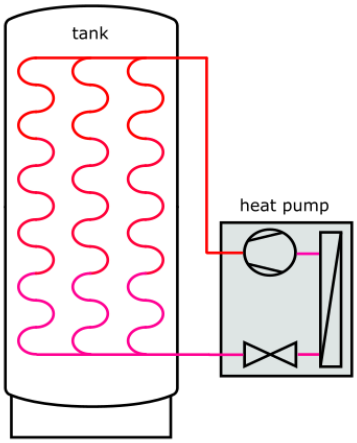

Figure 2: Alternative heat pump storage concept with condenser integrated into the storage tank

Figure 3 shows the detailed alternative heat pump storage tank concept. Two consumer circuits are connected to the tank, DHW at the top and space heating at the bottom, allowing the tank to be divided into two zones. In the upper zone, water is to be stored at a temperature level for DHW (55 °C – 70 °C), which is supplied hygienically via a heat exchanger. The lower zone is used to store space heating (30 °C – 55 °C). The tank concept uses the effect that warm water has a lower density than cold water and therefore collects in the top of the tank. The upper area of the tank is only used for DHW preparation, for which heat is extracted from the top part of the tank via the plate heat exchanger as required and reintroduced at the bottom of the tank. In this way, the DHW is only heated when it is actually needed.

The heat pump should have a heating capacity of 10 kW at operating point B0W35. Figure 3 shows an example of the operating point and illustrates the advantage of the concept. The refrigerant is compressed in the compressor and enters the condenser in the tank superheated at a temperature of around 70 °C, transfers the heat to the water in the upper part of the tank and thus heats the DHW. The refrigerant then condenses at 40 °C and heats the space heating water. In the lower part of the condenser, it is assumed that the refrigerant is subcooled by 5 K. This means that if there is a constant heat demand from the building, domestic hot water can be produced in parallel without a special DHW mode.

The storage tank has a volume of 780 l, of which approx. 320 l is for the DHW zone and approx. 460 l for the space heating zone. The tank has a diameter of 770 mm and a height of 1900 mm. The designed heat pump should have a maximum heating capacity of 14 kW at max. compressor speed and a nominal heating capacity of 10 kW, for which a variable speed-controlled 42cc compressor was selected.

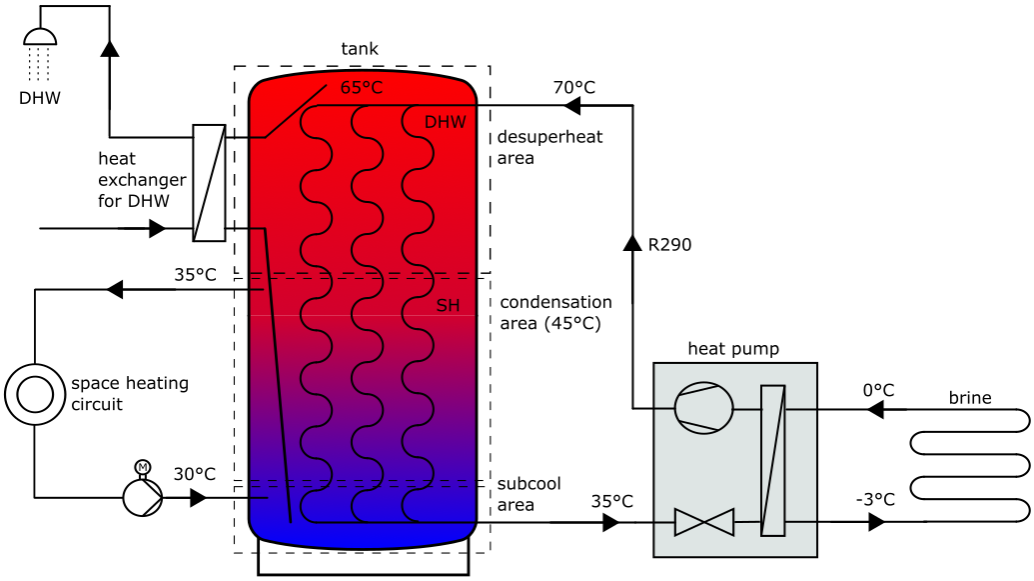

Figure 3: Heat pump storage concept at a typical operation point

The condenser being integrated in the storage tank has the advantage that no additional hydraulics are required to load the storage tank. This could save time when installing the heat pump in the building. Another advantage is the loading of the storage tank; heat is fed directly into the storage tank at the required point and the concept of a simple combination storage tank can therefore be implemented without complex storage tank installations such as stratification diverters or separators. Furthermore, an increase in efficiency is expected during operation in the building if the heat pump provides both space heating and DHW.

As part of the research project (HPPVT40), two different condenser storage tank concepts are being investigated. The efficiency of the heat pump, the refrigerant charge, the target temperatures in the storage tank and the heat up time of the tank are to be investigated using simulations and experiments. The design and thus the technical implementation of the concepts are also the focus of the investigations.

As the refrigerant R290 is to be used, reducing the charge is an important design criterion for the entire concept. To achieve this, the internal volume of the heat exchanger should be as small as possible but the external surface area as large as possible. A large external surface area fully compensates for the expected lower heat transfer coefficient during free convection. As part of a market research, various suppliers were compared with each other regarding the available geometries of finned tube heat exchangers. Figure 4 shows one example. A finned tube with an internal diameter of 6.5 mm, a fin height of 5 mm and a heat transfer surface of 0.197282 m²/m was selected. This is intended to increase the external surface area while reducing the internal volume of the condenser.

The second condenser storage tank option is a heat exchanger that is attached to the outside of the storage tank (mantle heat exchanger), whereby either a tube is wrapped around the storage tank mantle (Deutz et al., 2018) or an additional self-contained jacket is attached (L. J. Shah, 1999). These variants are used for storage tanks up to a volume of 800-1000 l, as otherwise the heat exchanger surface area is limited in relation to the storage tank volume and a heat exchanger installed in the storage tank is more advantageous (L. J. Shah, 1999). The disadvantage of such systems, however, is that there is an additional thermal resistance between the heat exchanger and the storage tank mantle. For this reason, the heat exchanger is to be integrated directly into the mantle as a pillow-plate heat exchanger as part of the innovative approach. Pillow-plate heat exchangers are mainly used in process technology as bundles in containers or in food technology as container walls (Tuber, 2018). An exemplarity design of the technology is shown in Figure 5. In cooperation with a heat exchanger manufacturer, a corresponding concept was developed, which provides a heat exchanger with the dimensions [2420 x 1500 x 4] mm and simultaneously functions as a storage mantle and condenser. For this purpose, two stainless steel plates were placed on top of each other and joined by laser welding. The flow paths were defined and then "inflated" using compressed air.

Figure 4: Example of a finned tube heat exchanger (*LASERFIN Rippenrohre - Schmöle*, 2024)

Figure 5: Example of a Pillow-Plate (BTH Import Stal, 2020)

3. MODELING OF THE SYSTEM

Modelica, the object-oriented programming language in Dymola is used to model the heat pump and the storage tank. The Modelica standard library (version 4.0.0), the external database TIL-Suite (version 3.13.0) and the add-on HeatStorage (version 3.13.0) from TLK-Thermo GmbH ("TIL Suite," 2023) are used. The existing component models were adapted and the fluid property data of the refrigerant R290 based on the external library Refprop (version 10.0). Since the explanations in this paper focus on the condenser storage tank system, the approach to the simulation of the other components is only briefly describe. The aim of the simulation is to map the condensor with regard to refrigerant charge, thermal performance and achievable temperatures in the top of the tank for DHW.

3.1 Compressor

The compressor model of the TIL-Suite requires the specification of the volumetric efficiency, the isentropic efficiency, and the effective isentropic efficiency (taking into account the electrical efficiency). These key figures are determined from AHRI coefficients provided by the manufacturer for various speeds for the used compressor. The AHRI coefficients can be used to map the operating behavior of compressors and are also used to calculate the mass flow of the refrigerant, the electrical power to be applied by the compressor and the heating capacity of the system (Prosser, 2020). The electrical power, mass flow and heat output are linearly interpolated between the given compressor speeds.

3.2 Evaporator

The evaporator is designed as a plate heat exchanger. A 35% ethylene glycol/water mixture is used as the secondary fluid, as negative evaporation temperatures can occur. To map the number of plates and the properties of the evaporator as accurately as possible, manufacturer data (geometric data and performance points) were fitted. The correlations according to Longo et al. (Longo et al., 2015) are used to calculate the heat transfer. The heat transfer and pressure loss of the secondary fluid were modeled with the correlations from the VDI Heat Atlas (Stephan et al., 2019). The simulation results showed that the COP is no longer strongly influenced above a plate number of 34. In addition, the evaporator should not be oversized due to the choice of refrigerant.

3.3 Condenser and Storage Tank

The condenser with storage tank is modeled in two versions (finned tube heat exchanger and mantle heat exchanger) With the HeatStorages add-on from TLK-Thermo GmbH. It is modelled one-dimensionally with a discretization over the height (see Figure 6). Each layer/cell "i" has the same volume and is assumed to be fully mixed. There is no radial temperature gradient in the model. Figure 7 shows the liquid state in a storage cell i (Liquid) with the two heat exchanger options. The condenser is modeled as a tube in both cases. Depending on whether the mantle (left tube) or finned tube (right tube) condenser is to be considered, the other one is deactivated in the code. Heat is transferred between the medium in the storage tank and the condenser via the HeatPort (red). Each storage cell has a LiquidPort (blue) and HeatPort to the cell above and below for energy and mass conservation.

Figure 6: Discretization of the storage tank in i=n cells over the tank height

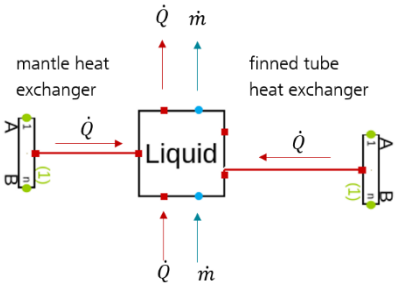

Figure 7: Modeling the tank cell with TIL-Suite

Using the TIL Suite, Deutz et al. (Deutz et al., 2018) investigated a Heat Pump Water Heater (HPWH) with air as the source and a 200 l storage tank for DHW with a mantle heat exchanger as a tube wrapped around the tank mantle with a length of 73 m and a diameter of 8.5 mm. Among other things, they concluded that a 1D-modeled storage tank provides sufficiently accurate results. They compared their modeled system with own experimental results and came to the result that the overall mean relative percentile error in instantaneous COP during heat up of the storage tank is 2 %. The deviations in the transient behavior were +/- 10 %. Hiris et al. (Hiris et al., 2022) analyzed the thermal behavior of a seasonal storage tank for solar district heating. For this purpose, they also modeled the storage tank one-dimensionally, assumed ideal mixing and compared the results with measured values from the literature. The storage tank had a volume of 22'829 m³ and storage temperatures between 30 °C and 90 °C were considered. They concluded that the difference between the temperatures predicted by the model and the actual temperatures was less than 2.35 K. Heinz et al. (Heinz et al., 2016) modeled a heat pump storage tank combination whereby the storage tank, with a volume of 685 l was also modeled one-dimensionally. The mean square error in the storage tank temperature between simulations and measured values was <1 K, which is why they came to the conclusion that the 1D approach provides reliable results. The literature research showed that a 1D-modeled storage tank provides sufficiently accurate results, which is why the 1D approach is also being pursued for this research project.

3.4 Finned Tube to Water Heat Transfer

As described the internal heat exchanger is designed as a finned tube with an internal diameter of 6.5 mm to achieve the lowest possible refrigerant charge and a fin height of 5 mm, to achieve a larger surface area on the outside compared to a smooth tube.

Relatively few research results are available in the literature on the free convection of water on finned tube surfaces. Thess and Kaiser (Thess & Kaiser, 2019) also describe the sparse data on natural convection around horizontal finned tubes in the VDI Heat Atlas (Stephan et al., 2019), but they derive a Nusselt correlation (Nu) shown in Equation 1 from the available data. The parameters are the Rayleigh number Ra, the fin pitch b and the core tube diameter d. The sum of the core tube diameter and the simple fin height serves as the characteristic length for the heat transfer coefficient.

$$\mathrm{Nu} = 0{,}24 * (\mathrm{Ra} * \frac{b}{d})^{\frac{1}{3}} \tag{1}$$

The average surface temperature of the core tube is used to determine the Rayleigh number. The equation was developed from measurement data for air, which is in contrast to the application with water. It is valid in the range of $10^3 < \mathrm{Ra} < 10^7$. Berkel et al. (Berkel et al., 1984) investigated the free convection on a horizontal finned tube in water and formed a Nusselt correlation, which, however, is only valid for the two finned tubes under consideration. For this reason, the Nusselt correlation according to Thess and Kaiser (Thess & Kaiser, 2019) is used (Equation 1).

3.5 Mantle to Water Heat Transfer

The defined channels of the mantle heat exchanger are integrated as meanders over the entire height of the tank mantle. The distance between the channels is 16.5 mm. The literature often refers to two correlations for calculation of the heat transfer between the tank mantle and the storage medium. The correlation according to Churchill and Chu (Churchill & Chu, 1975), which can also be found in the VDI Heat Atlas, is widely used. The mantle height serves as the characteristic length for Ra.

$$\mathrm{Nu} = \left(0.825 + \frac{0.387 * \mathrm{Ra}^{1/6}}{(1 + (0.492/\mathrm{Pr})^{9/16})^{8/27}}\right)^2 \quad (2)$$

The correlation according to Shah (L. J. Shah, 2001) was developed specifically for a solar storage tank with a mantle heat exchanger, but only in conjunction with a storage tank volume of 170 l. The storage tank considered in this work has a volume of 780 l and is therefore significantly larger, which is why the correlation according to Churchill and Chu is used. The area on the tank mantle where there is no channel still functions as a heat exchanger. This area is assumed to be a fin of the pillow plate concept, therefore the efficiency η_R according to VDI Wärmeatlas (Stephan et al., 2019). The heat transfer coefficient α on the mantle is calculated with the Nusselt correlation from Equation 2, the thermal conductivity λ of the tank material, the material thickness s, and the fin height h are used.

$$\eta_f = \frac{\tanh(m * h)}{m * h} \quad (3)$$

with

$$m = \sqrt{\frac{\alpha}{\lambda * s}} \quad (4)$$

3.6 Heat Transfer in the Condenser

In the condenser, the refrigerant changes its aggregate state from gas to liquid. Depending on the state of the refrigerant, different correlations are used for heat transfer: The single-phase heat transfer is calculated in the range of 2300 < Re < 10000 according to Gnielinski's and in the range of Re > 10000 according to Dittus-Boelter, both equations can be found in the VDI Heat Atlas (Stephan et al., 2019). The condensation model according to Shah (M. M. Shah, 1979) is used for condensation in the coiled tube, as the model has a wide range of validity for horizontal, vertical and inclined tubes. Ye and Li (Ye & Li, 2019), for example, investigated a DHW heat pump (HPWH) and modeled the two-phase heat transfer according to Shah (1979), but assumed a 1.16 - 1.43 times higher heat transfer coefficient compared to the horizontal tube due to the coil of the heat exchanger based on (Prabhanjan et al., 2002).

$$\alpha = \alpha_l * \left[(1-x)^{0,8} + \frac{3{,}8x^{0,76} * (1-x)^{0,04}}{{p_r}^{0,38}}\right] \quad (5)$$

with

$$\alpha_l = 0.023\ Re_l^{0.8} * Pr_l^{0.4} * \frac{\lambda_l}{d} \quad (6)$$

$$p_r = \frac{p}{p_{crit}} \quad (7)$$

Here, α is the heat transfer coefficient during condensation, α_l is the heat transfer coefficient of the liquid refrigerant according to Dittus-Boelter. The reduced pressure p_r and the vapor content x are also included in the calculation. Another model for condensation in tubes is the model according to Xiao and Hrnjak (Xiao & Hrnjak, 2016), who investigated a HPWH in which the condenser was wrapped around the storage tank as a tube. The model is valid for horizontal tubes. Another possibility is to consider the condensation behavior in tube coils, such as by Wongwises and Polsongkram (Wongwises & Polsongkram, 2006). However, this model is very sensitive to the coil diameter. Preliminary investigations into the condensation models have shown that the lowest heat transfer coefficients are calculated according to Xiao and Hrnjak (2016) and the highest according to Wongwises and Polsongkram (2006). Since the present application does not use a horizontal tube, but a higher heat transfer coefficient can be assumed due to the coil, the correlation according to Shah (1979) is used.

The pressure loss during condensation is calculated according to Müller-Steinhagen and Heck (Müller-Steinhagen & Heck, 1986). And the single-phase pressure loss according to Konakov from the VDI Heat Atlas (Stephan et al., 2019). Due to the use of the pillow plate heat exchanger, whose channel has a hydraulic diameter of 1.72 mm, a literature research was carried out to legitimize the use of the correlation. Cavallini et al. (Cavallini et al., 2006) came to the conclusion that the correlation according to Müller-Steinhagen and Heck is suitable for pressure loss investigations in mini-channels with a hydraulic diameter between 1 - 4.91 mm.

4. SIMULATION RESULTS

4.1 Finned Tube Heat Exchanger

The used finned tube has an inner diameter of only 6.5 mm. To estimate the potential efficiency, additional simulations were also carried out with two or three tube coils connected in parallel, which then had a correspondingly lower pitch of the coil, in addition to the single coiled finned tube. The single coil had a height of 1.5 m in the tank with a coil pitch of 0.0262 m. The two parallel tubes also had a height of 1.5 m, but a coil pitch of 0.0525 m - with three tubes, the height of the individual coils is also 1.5 m with a coil pitch of 0.0791 m.

The achievable tank top temperatures are decisive for DHW preparation and are shown in Figure 8 at a constant heating capacity of 10 kW and a heating circuit temperature of 35 °C versus the heat exchanger surface area. For one tube, the achievable tank top temperature is between 81 °C and 87 °C, for two parallel tubes between 71 °C and 79 °C and for three parallel tubes between 68 °C and 81 °C. All temperatures reached are sufficient to provide DHW. As the heat exchanger area increases, the storage head temperature falls before rising again after a minimum, which is due to the increasing pressure loss of the condenser with increasing tube length. Before the minimum, the influence of the increasing heat exchanger surface is dominant. Figure 9 shows the saturation temperature calculated from the pressure at the end of compression. The curve is comparable to that of the tank top temperature. As the heat exchanger surface area increases, the condensation temperature decreases, as only a smaller temperature gradient is required for heat transfer. For example, the condensation temperature for one tube is between 50 °C and 56 °C, for two tubes between 42 °C and 48 °C and for three tubes between 39 °C and 50 °C in order to achieve a heating water flow temperature of 35 °C in each case. After a minimum, the condensation temperature rises again, as does the tank top temperature. This is due to the increasing pressure loss with increasing tube length, which increasingly dominates in comparison to the larger heat exchanger surface.

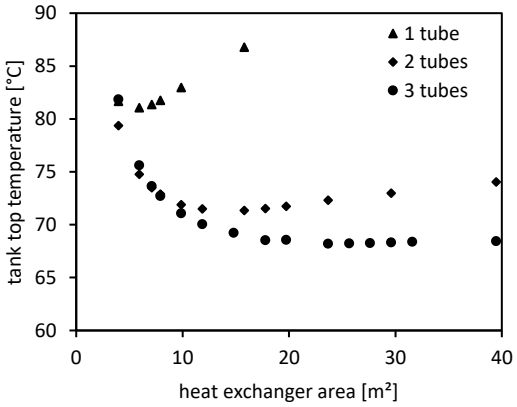

Figure 8: Tank top temperature for one, two and three parallel tubes

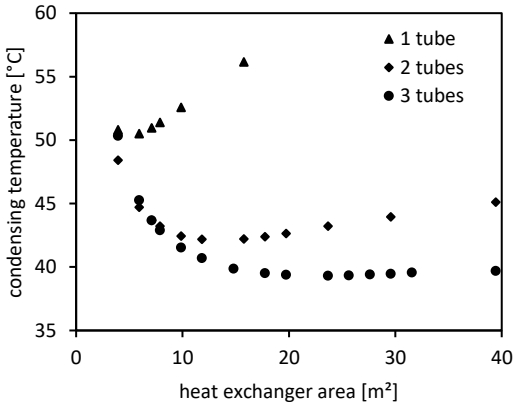

Figure 9: Saturation temperature for one, two and three parallel tubes

The COP shown in Figure 10 (at operating point B0W35 and 10 kW) is the inverse of the curve for the tank top and condensation temperatures. The highest COP, shown in red in each case, is 3.97 for three parallel tubes with a heat exchanger area of 29.5 m², which corresponds to a length of 150 m. For two parallel tubes, the maximum COP is 3.83 for an area of 17.76 m² and 3.45 for one tube with an area of 7.1 m².

The design with three parallel tubes was chosen to ensure the most even heat input possible into the storage tank. The coil diameter (200 mm) was selected so that the distance between the coils and the radius to the tank wall is the same.
Table 1 shows the refrigerant charge of the other components and the planned total heat pump charge. This results in a theoretical available refrigerant charge for the condenser of 180 g, which is achieved with a condenser tube length of 45 m and a COP of 3.7. Accordingly, a 6.8 % lower COP would have to be accepted for a reduction in the charge respectively charge restriction for this case.

Table 1: Estimated refrigerant charge of the components and the target heat pump charge

Component	Heat Pump target	Compressor	Evaporator	Pipes	*Condenser*
Charge [g]	500	110	140	70	*180*

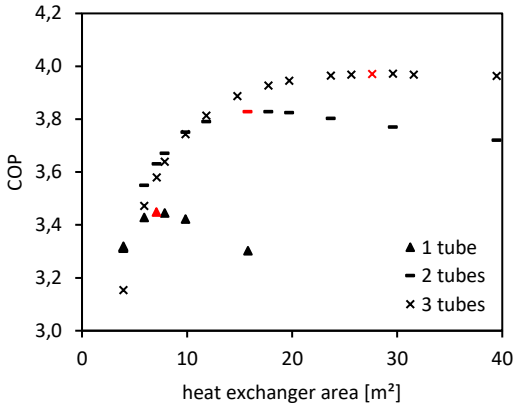

Figure 10: COP of one, two and three parallel tubes versus the heat exchanger surface

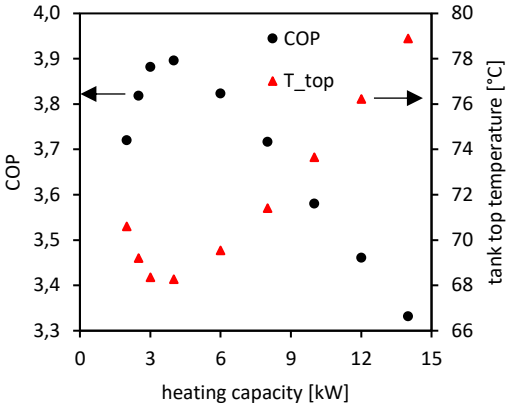

Figure 11: COP (primary axis) and tank top temperature (secondary axis) versus the heating capacity for 3 parallel tubes and 36 m overall length

Consultations with the heat exchanger manufacturer also revealed that the maximum pipe length to be coiled is 12 m (in total with three parallel tubes 36 m, corresponds to 7.1 m² heat exchanger area). This length would result in a COP of 3.58 with a refrigerant charge of 140 g. This option is now being implemented in a test bench and will be investigated experimentally over the next months. Figure 11 shows the COP of the system with the selected condenser option over the heating capacity. The curve reflects the isentropic efficiency of the compressor. The optimum COP of 3.9 is at a partial load of 4 kW; the lowest storage head temperature of 68 °C is also achieved at this operating point (Figure 11).

4.2 Mantle Heat Exchanger

The manufacturing process for the pillow plate resulted in fewer degrees of freedom for the mantle heat exchanger. The total length of the channels integrated into the mantle is 48 m and the total mantle area is 3.636 m². Figure 12 shows the COP versus the number of parallel channels at operating point B0W35 and 10 kW heating capacity. All designs with the different number of parallel channels have the same overall length of the channels of 48 m. This results in an optimum COP of 3.37 with 6 parallel channels. In contrast to the finned tube, the heat exchanger surface could not be varied, but the influence on the COP results from the changed flow characteristic of the refrigerant. As the number of parallel channels increases, the refrigerant mass flow is divided, which reduces the flow velocity, the Reynolds number, the heat transfer coefficient, and also the pressure loss. However, as the thermal resistance at the transition to the tank medium is limiting, the COP only varies by approx. +/- 0.1. The achievable tank top temperatures are between 78 °C and 85.5 °C.

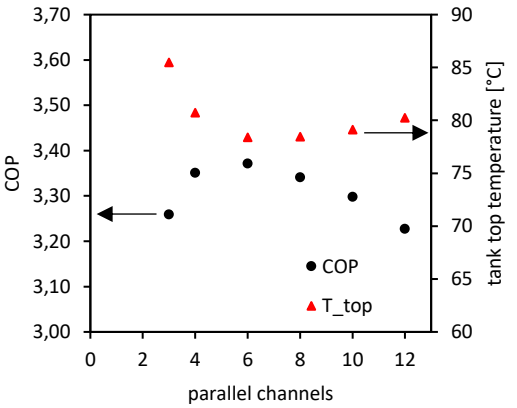

Figure 12: COP (primary axis) and tank top temperature (secondary axis) versus the number of parallel channels at B0W35 and 10kW heating capacity

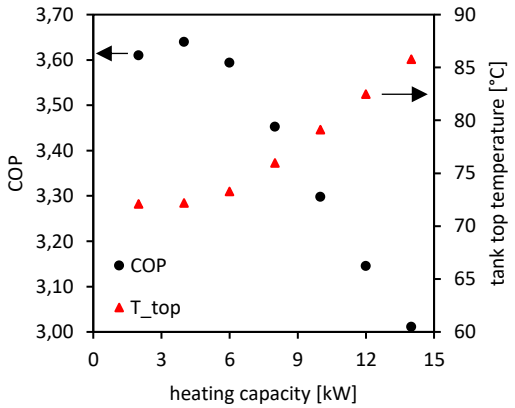

Figure 13: COP (primary axis) and tank top temperature (secondary axis) versus the heating capacity for B0W35 and 10 parallel channels

Due to the uncertainties regarding the geometry of the channels caused by the manufacturing process, 10 parallel channels were selected in consultation with the manufacturer. Figure 13 shows the COP values and achievable tank top temperatures versus the heating capacity range by changing the compressor speed for the implemented variant with 10 parallel channels. The COP at 10 kW is 3.30 and the achievable tank top temperature is 79 °C. The highest COP of 3.64 is achieved at 4 kW heating capacity. In this case the refrigerant charge of the condenser calculated with 200 g, but this value must be confirmed with the test bench due to the uncertain volume of the channels.

4. CONCLUTION

The article presented a heat pump storage concept for the simultaneous provision of space heating and domestic hot water. For this purpose, a simulation model consisting of the heat pump and the storage tank, which was modeled one-dimensionally, was presented. In addition, two condenser variants implemented in the storage tank were presented in order to reduce the refrigerant charge, among other things. The simulation results show that sufficiently high tank top temperatures of 73 °C for the finned tube, respectively 79 °C for the mantle heat exchanger at the operating point B0W35 and 10 kW heating capacity can be achieved. The associated COP at the given operation point is 3.58 for the finned tube, respectively 3.30 for the mantle heat exchanger. To validate the simulation model, both variants are set up in a heat pump test rig and will be experimentally investigated in the laboratory at Fraunhofer ISE, Germany.

NOMENCLATURE

α	Heat Transfer Coefficient	(W/(m²K))
b	fin pitch	(m)
COP	Coefficient of Performance	(-)
d	Diameter	(m)
λ	thermal conductivity	(W/(mK))
Pr	Prandtl Number	(-)
Nu	Nusselt Number	(-)
Ra	Rayleigh number	(-)
Re	Reynold Number	(-)
p	pressure	(Pa)
x	Thermodynamic vapor quality	(-)

Subscript

$crit$	critical
l	liquid
f	fin
r	reduced

REFERENCES

Berkel, H., Mitra, N. K., & Fiebig, M. (1984). Experimentelle Untersuchung des Wärmeüberganges durch freie Konvektion an waagerechten Rippenrohren in einem zylindrischen Behälter. *Wärme- Und Stoffübertragung*, *18*(3), 167–173. https://doi.org/10.1007/BF01466348

BTH Import Stal. (2020, December 15). *Pillow Plate - Heiz- und Kühlmäntel - BTH Import Stal*. https://bth.pl/de/dienstleistungen/pillow-plate-heiz-und-kuhlmantel/

Cavallini, A., Doretti, L., Matkovic, M., & Rossetto, L. (2006). Update on Condensation Heat Transfer and Pressure Drop inside Minichannels. *Heat Transfer Engineering*, *27*(4), 74–87. https://doi.org/10.1080/01457630500523907

Churchill, S. W., & Chu, H. H. (1975). Correlating equations for laminar and turbulent free convection from a vertical plate. *International Journal of Heat and Mass Transfer*, *18*(11), 1323–1329. https://doi.org/10.1016/0017-9310(75)90243-4

Deutz, K. R., Charles, G.-L., Cauret, O., Rullière, R., & Haberschill, P. (2018). Detailed and dynamic variable speed air source heat pump water heater model: Combining a zonal tank model approach with a grey box heat pump model. *International Journal of Refrigeration*, *92*, 55–69. https://doi.org/10.1016/j.ijrefrig.2018.05.022

Günther, D., Wapler, J., Langner, R., Helmling, S., Miara, M. Dr.-Ing., Fischer, D. Dr.-Ing., Zimmermann, D., Wolf, T., & Wille-Hausmann, B. Dr.-Ing. (2020). *Wärmepumpen in Bestandsgebäuden: Ergebnisse*

aus dem Forschungsprojekt "WPsmart im Bestand". Fraunhofer-Institut für Solare Energiesysteme ISE. https://wp-monitoring.ise.fraunhofer.de/wpqs-im-bestand/download/Berichte/BMWi-03ET1272A-WPsmart_im_Bestand-Schlussbericht.pdf

Haller, M. Y., Haberl, R., Mojic, I., & Frank, E. (2014). Hydraulic Integration and Control of Heat Pump and Combi-storage: Same Components, Big Differences. *Energy Procedia*, *48*, 571–580. https://doi.org/10.1016/j.egypro.2014.02.067

Heinz, A [A.], Lerch, W [W.], & Heimrath, R [R.] (2016). Heat pump condenser and desuperheater integrated into a storage tank: Model development and comparison with measurements. *Applied Thermal Engineering*, *102*, 465–475. https://doi.org/10.1016/j.applthermaleng.2016.04.010

Hiris, D. P., Pop, O. G., & Balan, M. C. (2022). Analytical modeling and validation of the thermal behavior of seasonal storage tanks for solar district heating. *Energy Reports*, *8*, 741–755. https://doi.org/10.1016/j.egyr.2022.07.113

LASERFIN Rippenrohre - Schmöle. (2024, April 25). https://schmoele.de/de/produkte/rippenrohre/laserfin/

Lerch, W [Werner], Heinz, A [Andreas], & Heimrath, R [Richard] (2014). Evaluation of Combined Solar Thermal Heat Pump Systems Using Dynamic System Simulations. *Energy Procedia*, *48*, 598–607. https://doi.org/10.1016/j.egypro.2014.02.070

Longo, G. A., Mancin, S., Righetti, G., & Zilio, C. (2015). A new model for refrigerant boiling inside Brazed Plate Heat Exchangers (BPHEs). *International Journal of Heat and Mass Transfer*, *91*, 144–149. https://doi.org/10.1016/j.ijheatmasstransfer.2015.07.078

Müller-Steinhagen, H., & Heck, K. (1986). A Simple Friction Pressure Drop Correlation for Two-Phase Flow in Tubes: eine einfache Gleichung zur Berechnung des Reibungsdruckverlusts bei der Zweiphasenströmung in Rohren.

Tuber, M. (2018). *Analysis of fluid dynamics and heat transfer in pillow-plate heat exchangers* [, UB-PAD - Paderborn University Library]. DataCite.

Prabhanjan, D. G., Raghavan, G., & Rennie, T. J. (2002). Comparison of heat transfer rates between a straight tube heat exchanger and a helically coiled heat exchanger. *International Communications in Heat and Mass Transfer*, *29*(2), 185–191. https://doi.org/10.1016/S0735-1933(02)00309-3

Prosser, J. (2020). *ANSI/AHRI Standard 540: Performance Rating of Positive Displacement Refrigerant Compressors.* Air-Conditioning, Heating, and Refrigeration Institute.

Shah, L. J. (1999). *Investigation and modelling of thermal conditions in low flow SDHW systems*. *Rapport / Institut for Bygninger og Energi, Danmarks Tekniske Universitet: R/034*. IBE, Institut for Bygninger og Energi, Danmarks Tekniske Universitet.

Shah, L. J. (2001). Heat transfer correlations for vertical mantle heat exchangers. *Solar Energy*, *69*, 157–171. https://doi.org/10.1016/S0038-092X(01)00039-1

Shah, M. M. (1979). A general correlation for heat transfer during film condensation inside tubes. *International Journal of Heat and Mass Transfer*, *22*(4), 547–556. https://doi.org/10.1016/0017-9310(79)90058-9

Stephan, P., Kabelac, S., Kind, M., Mewes, D., Schaber, K., & Wetzel, T. (2019). *VDI-Wärmeatlas*. Springer Berlin Heidelberg. https://doi.org/10.1007/978-3-662-52989-8

Thess, A., & Kaiser, R. (2019). F2 Wärmeübertragung bei freier Konvektion: Außenströmungen. In *VDI-Wärmeatlas* (pp. 763–772). Springer Vieweg, Berlin, Heidelberg. https://doi.org/10.1007/978-3-662-52989-8_38

TIL Suite (Version 3.10.0) [Computer software]. (2023). TLK Thermo GmbH. https://www.tlk-thermo.de/

Wongwises, S., & Polsongkram, M. (2006). Condensation heat transfer and pressure drop of HFC-134a in a helically coiled concentric tube-in-tube heat exchanger. *International Journal of Heat and Mass Transfer*, *49*(23-24), 4386–4398. https://doi.org/10.1016/j.ijheatmasstransfer.2006.05.010

Xiao, J., & Hrnjak, P. (2016). Heat transfer and pressure drop of condensation from superheated vapor to subcooled liquid. *International Journal of Heat and Mass Transfer*, *103*, 1327–1334. https://doi.org/10.1016/j.ijheatmasstransfer.2016.08.036

Ye, Q., & Li, S. (2019). Investigation on the performance and optimization of heat pump water heater with wrap-around condenser coil. *International Journal of Heat and Mass Transfer*, *143*, 118556. https://doi.org/10.1016/j.ijheatmasstransfer.2019.118556

ACKNOWLEDGEMENT

The study presented in this paper received funding from the German Federal Ministry of Economic Affairs and Climate Action (BMWK) under the grant agreement number FKZ 03EN4016A (HPPVT40).